



SPE 89866

A Comparative Study of Laboratory Techniques for Measuring Capillary Pressures in Tight Gas Sands

K.E. Newsham, SPE, Apache Corp., J.A. Rushing, SPE, Anadarko Petroleum Corp., P.M. Lasswell, OMNI Laboratories Inc., J.C. Cox, SPE, Texas Tech University, and T.A. Blasingame, SPE, Texas A&M University

Copyright 2004, Society of Petroleum Engineers Inc.

This paper was prepared for presentation at the SPE Annual Technical Conference and Exhibition held in Houston, Texas, U.S.A., 26–29 September 2004.

This paper was selected for presentation by an SPE Program Committee following review of information contained in a proposal submitted by the author(s). Contents of the paper, as presented, have not been reviewed by the Society of Petroleum Engineers and are subject to correction by the author(s). The material, as presented, does not necessarily reflect any position of the Society of Petroleum Engineers, its officers, or members. Papers presented at SPE meetings are subject to publication review by Editorial Committees of the Society of Petroleum Engineers. Electronic reproduction, distribution, or storage of any part of this paper for commercial purposes without the written consent of the Society of Petroleum Engineers is prohibited. Permission to reproduce in print is restricted to a proposal of not more than 300 words; illustrations may not be copied. The proposal must contain conspicuous acknowledgment of where and by whom the paper was presented. Write Librarian, SPE, P.O. Box 833836, Richardson, TX 75083-3836, U.S.A., fax 01-972-952-9435.

Abstract

This paper presents results from a laboratory study comparing capillary pressure measurement techniques for tight gas sands. Included in our evaluation are the more traditional high-speed centrifuge and high-pressure mercury injection methods as well as the less conventional high-pressure porous plate and vapor desorption techniques. The results of our study show significant differences between the mercury injection data and composite capillary pressure curves constructed with data from the other three methods. Consequently, we have concluded that high-pressure mercury injection can be used to quantify pore size distribution, but often inaccurately characterizes capillary pressures, particularly at the irreducible water saturation. Moreover, our study suggests that a composite capillary pressure curve constructed from a combination of the vapor desorption data for the low water saturation range and high-speed centrifuge or high-pressure porous plate data for the high saturation range provides the most accurate capillary pressures for tight gas sands.

Introduction

Tight gas sands constitute a significant percentage of the domestic natural gas resource base and offer tremendous potential for future reserve growth and production. Since tight gas sands often exhibit unique gas storage and producing characteristics, effective exploitation requires accurate description of key reservoir parameters, particularly capillary pressures to quantify the vertical water saturation distribution and resource-in-place. Furthermore, the combination of low connate water saturations and high capillary pressures characteristic of many low-permeability systems often precludes use of most conventional laboratory measurement techniques that are most applicable in reservoirs with higher permeabilities and porosities.

To date, no comprehensive evaluation of capillary pressure measurement techniques for tight gas sands has been published in the petroleum literature. Accordingly, this paper presents a comparative study of all current laboratory methods, including the more traditional high-speed centrifuge and high-pressure mercury injection methods and the less conventional high-pressure porous plate and vapor desorption techniques.

Twenty-five core samples, taken from wells producing in the Lower Cotton Valley/Bossier tight gas sands in the East Texas and North Louisiana Salt Basins, are used in the study. Core properties, representing most of the entire range of productive sands, include porosities from about 2% to 14% and Klinkenberg-corrected permeabilities ranging from about 0.0005 md to 0.5 md. Water saturations, which typically range from 5% to 60% in these sands, are also associated with very high capillary pressures.^{1,2}

Theoretical Aspects of Capillarity in Porous Media

A wetting fluid or liquid is retained within a porous medium by two types of forces—surface forces holding the liquid as a molecular film completely covering the rock surfaces, and capillary forces holding the liquid as a bulk fluid with curved interfaces separating the liquid and vapor phases.³ If the liquid appears as a bulk fluid phase that completely and continuously coats the rock surfaces, then capillary pressure can be computed in terms of the liquid surface curvature with the Young-Laplace⁴ equation given by

$$P_c = \frac{2\sigma \cos \theta}{r} \dots\dots\dots(1)$$

where

- P_c = capillary pressure
- σ = surface tension
- θ = contact angle
- r = pore throat radius

Equation (1), which was derived from the physics of capillary rise in a tube, reflects the balance between capillary and gravitational forces. Moreover, the Young-Laplace equation is an equilibrium-state equation that implicitly assumes the presence of a continuous liquid or wetting phase coating the rock surfaces. For most conventional hydrocarbon reservoirs,

this assumption is valid and Equation (1) is applicable. However, for some tight gas sands characterized by ultra-low water saturations in which the wetting phase is discontinuous (*i.e.*, sub-irreducible water saturations),^{1,2} the Young-Laplace equation may be inappropriate for computing capillary pressures.

Alternatively, Melrose,⁵ Collins,³ and Calhoun⁶ have derived a relationship between capillary pressure and vapor pressure for a pore system containing water in equilibrium with its vapor. Their derivation is based on the observation from Lord Kelvin⁷ that the partial pressure of a vapor in equilibrium with the bulk liquid is a function of the curvature of the vapor-liquid interface. Since the liquid interface curvature depends on saturation, then it follows that the partial pressure of a vapor is also dependent on the liquid saturation. Written in terms of partial pressures, capillary pressure can be computed from a modified form of the Kelvin equation as

$$P_c = \ln \left(\frac{p_{v1}}{p_{v2}} \right) \frac{RT}{V_m} \dots\dots\dots (2)$$

where

- P_c = capillary pressure
- p_{v1} = partial vapor pressure for brine within the pores
- p_{v2} = partial vapor pressure for equilibrating salt solution
- R = Universal gas constant
- T = absolute temperature
- V_m = molar volume of water

Equation (2) can also be rewritten in terms of relative humidity as follows:

$$P_c = - \frac{\ln (RH/100) RT}{V_m} \dots\dots\dots (3)$$

where *RH* is the relative humidity of the water vapor. Equations (2) and (3) describe mathematically the effect of changes in vapor pressure and relative humidity, respectively, on the capillary pressure computations. Melrose⁸ has proven that Equations (2) and (3) are valid for describing capillary pressures in reservoirs having very low water saturations. Moreover, references 2 and 6-10 have shown how capillary pressures may be measured using a vaporization or vapor desorption process that incorporates Equations (2) and (3).

Figure 1 is a conceptual model showing the drainage path as water saturation is decreased by vaporization processes. From pore throats 'a' through 'c', enough water is present to maintain a continuous wetting phase. Within these conditions, the cohesive force (attraction of like molecules) of the wetting phase is greater than the adhesive force created at the contact between the rock and the wetting phase. During the transition from 'b' to 'c', the adhesion force will cause the water molecules to spread across the maximum grain surface area, down to a single molecular layer. The Young-Laplace equation is still appropriate through these stages since the water is still in a continuous distribution across the rock

surface and cohesion forces are still significant. At this point the adhesion and cohesion forces are nearly balanced.

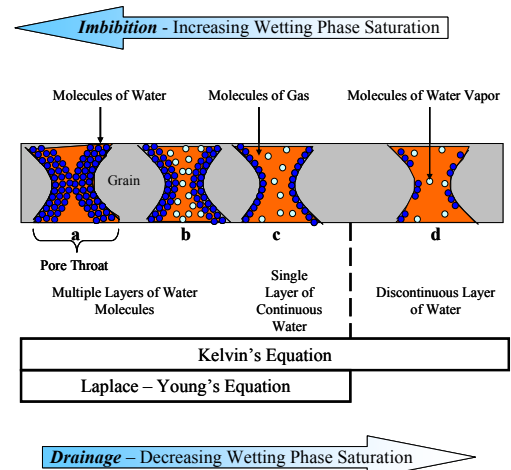


Fig. 1—Conceptual physical model illustrating the vapor desorption process and the saturation regions where each of the capillary pressure equations are most applicable.

As the saturation state is reduced further by vapor desorption, the single layer of water molecules is broken, resulting in a non-continuous wetting phase. At this point, the adhesion force is probably greater than the cohesion force of the water molecules. Effectively, the rock no longer has a continuous wetting phase, and the water saturation is in a sub capillary-equilibrium state.^{1,2} Under these conditions, the Kelvin equation, rather than the Young-LaPlace equation, is most appropriate. Parenthetically, the Kelvin equation is valid for all saturation ranges, but is most applicable in the low saturation region. Hence, the vapor desorption technique for measuring capillary pressure in tight gas sands with ultra-low water saturation is thought to be the superior method.

Overview of Capillary Pressure Measurement Techniques Used in Study

In this section, we review the three primary capillary pressure measurement techniques used by the petroleum industry, including the porous plate, centrifuge, and high-pressure mercury injection. Although its use is less widespread, the vapor desorption method offers some advantages over the more conventional methods. Each of the measurement techniques is also applicable to very specific testing conditions and is often appropriate for specific types of reservoir rocks.

Porous Plate Method.⁹⁻¹² The principal component of the porous plate method is a permeable material having a uniform pore size distribution and containing pores of appropriate size such that the displacing fluid will not penetrate the membrane at some maximum pressure.⁴ In addition, the permeable material must have wetting characteristics such that the displaced fluid will completely wet the material surfaces and saturate the pores. Historically, ceramic has been used as the permeable material; however, plastic membranes have replaced ceramic to allow higher displacement pressures. Capillary pressures are computed from the pressure increases required to displace fluid from increasingly smaller pores and pore throats.

The primary advantage of the porous plate method is the ability to test porous material using 'native' fluids and 'native-state' rocks. Consequently, it is not necessary to clean and dry samples before testing, thereby reducing the risk of either changing the *in-situ* wettability or altering intrinsic rock properties. This advantage is quite important in rocks containing significant clays and shales. Also, the dynamics of the porous plate desaturation process most closely match those of the reservoir. Finally, the effects of evaporation and handling are minimized rendering very precise measurement of water saturation.

The primary disadvantage of the porous plate method is a limitation on the highest capillary pressure that can be achieved. The upper limit of capillary pressure is controlled by the size of the smallest pore throats in the membrane. Another significant limitation or disadvantage of the porous plate method is the long times required to reach equilibrium saturation levels. Both of these disadvantages limit using the porous plate method in tight gas sands.

Centrifuge Method.¹³⁻¹⁶ As the name implies, the centrifuge method desaturates a core sample by imposing a centrifugal force on the sample, thus forcing the mobile phase out. The centrifugal force is created by rotating or spinning the core at increasingly higher speeds. The principal advantage of the centrifuge is the ability to obtain capillary pressure data very quickly relative to the porous plate method. Furthermore, many high-speed centrifuges can now be operated at reservoir pressure and temperature conditions.

Similar to the porous plate method, the main disadvantage of the centrifuge method is the maximum pressure limitation. Most high-speed centrifuges are limited to a maximum capillary pressure of 1000 psi. Another concern with the centrifuge technique is the uncertainty as to the distribution of the wetting phase fluid within the plug. Irregular wetting phase distributions can cause capillary end effects.¹⁵

Additional problems include cavitation, liquid evaporation, and water volume hold-up. Cavitation occurs in gas-liquid systems when the air pressure is less than one atmosphere but the capillary pressure exceeds one atmosphere.¹⁶ Liquid evaporation during the test process will lower the computed water saturations. Conversely, water volume hold-up and low water volumes recovered will tend to increase the computed water saturations. Finally, we may be subject to measurement inaccuracies caused by very small displacement volumes typical of low-porosity tight gas sands.

High Pressure Mercury Injection Method.¹⁷ High-pressure mercury injection (MICP) involves injecting or forcing mercury into an evacuated core sample. The volume of mercury injected at each pressure step determines the non-wetting (*i.e.*, mercury) saturation. Unlike the porous plate technique, this method is very fast, often requiring only hours rather than days or weeks. Further, MICP is capable of attaining injection pressures as great as 60,000 psi, thus providing coverage of the entire range of water saturation and capillary pressure for both tight gas and high porosity, permeable rocks.

The disadvantages include the lack of a true wetting phase during testing. The test is performed on dry samples using

mercury as the non-wetting phase fluid and assuming air is the wetting fluid. This requires conversion to reservoir conditions using contact angle and surface tension inputs.

Additionally, the oil and gas industry lacks standards for correcting the apparatus for system compressibility at high pressures (*e.g.* blank corrections) resulting in water saturation/capillary pressure distribution measurement errors. Finally, use of the contact angle and surface tension scaling parameters may not be appropriate for rocks with ultra-low water saturations and high capillary pressures or rocks with slot type pores, common to tight gas sand reservoirs.⁸ High-pressure mercury injection is, however, an excellent tool for quantifying a rock's pore sizes and distribution.

Vapor Desorption Method.^{5,8,18-20} The fundamental principal of vapor desorption or vapor pressure lowering is the observation that the vapor pressure above a liquid's curved surface is a function of the liquid surface curvature.⁷ In addition, the capillary pressure is a function of the liquid surface curvature. As a result, both capillary pressure and vapor pressure lowering are functions of the liquid saturation in a porous medium. Capillary pressures, therefore, are calculated from lowering the vapor pressure by controlling the relative humidity in the rock pores.

Vapor pressure reduction can be controlled with humidity chambers where relative humidity and the subsequent saturation equilibrium is controlled with various concentrations of salts in a liquid solution.^{5,8,18-20} The primary advantage of this method is the ability to achieve very high capillary pressures as well as very low water saturations. Melrose^{5,8} used various salt solutions to decrease the vapor pressure on core samples in a humidity chamber, resulting in capillary pressures as high as 4,000 psi for an air/brine system.⁵ We have achieved air-water capillary pressures in excess of 10,000 psi and water saturations below 5%. As a result, this technique is especially suited for reservoir systems characterized by ultra-low water saturations and abnormally high capillary pressures like the Lower Cotton Valley/Bossier sands.¹

The vapor desorption measurement precision decreases, however, at very high relative humidity (>95%) which limits the lower limit of capillary pressure to a value of about 1000 psi. Consequently, a disadvantage of the vapor desorption technique is the inability to measure capillary pressures at high water saturations. Similar to the porous plate method, another limitation is the stabilization time, which typically may be several days or even weeks.

Laboratory Materials and General Procedure

Materials. Capillary pressures were measured on twenty-five core samples taken from four wells completed in the Lower Cotton Valley/Bossier tight gas sand plays in the East Texas and North Louisiana Salt Basins. We believe these sands are strongly water-wet, so most plugs were taken from whole cores obtained with an oil-base mud program in an attempt to quantify initial connate water saturations more accurately. Tables 1-4 list the core samples used in the laboratory measurements, their intrinsic properties, and the capillary pressure measurement technique evaluated in our study.

Table 1—Summary of Intrinsic Rock Properties for East Texas Field No. 1, Well No. 1

Sample No.	Effective Porosity (%)	Klinkenberg-Corrected Permeability (md)	Capillary Pressure Measurement Technique
2-20A	11.9	0.0870	HSC, VD, MICP
2-22A	11.2	0.0770	HSC, VD, MICP
2-29A	8.4	0.0300	HSC, VD, MICP
2-32B	7.5	0.0130	HSC, VD, MICP
2-39A	1.9	0.0055	HSC, VD, MICP
2-41A	8.7	0.0480	HSC, VD, MICP

Table 2—Summary of Intrinsic Rock Properties for East Texas Field No. 2, Well No. 1

Sample No.	Effective Porosity (%)	Klinkenberg-Corrected Permeability (md)	Capillary Pressure Measurement Technique
36	4.3	0.0027	HPPP, VD
49	10.3	0.0210	HPPP, VD, MICP
70	12.0	0.0073	HPPP, VD, MICP
211	11.8	0.0117	HPPP, VD
212	12.3	0.0221	HPPP, VD
218	6.7	0.0268	HPPP, VD

Table 3—Summary of Intrinsic Rock Properties for North Louisiana Field, Well No. 1

Sample No.	Effective Porosity (%)	Klinkenberg-Corrected Permeability (md)	Capillary Pressure Measurement Technique
1-26	5.3	0.0040	HPPP, HSC, VD, MICP
2-28	4.9	0.0006	HPPP, HSC, VD, MICP
2-32	8.4	0.0850	HPPP, HSC, VD, MICP
2-50	7.6	0.0009	HPPP, VD
3-17	13.8	0.1430	HSC, , VD
3-42	13.0	0.0410	HPPP, HSC, VD, MICP
4-18	8.7	0.0066	HSC, VD
4-44	9.8	0.027	HPPP, VD, MICP

Table 4—Summary of Intrinsic Rock Properties for North Louisiana Field, Well No. 2

Sample No.	Effective Porosity (%)	Klinkenberg-Corrected Permeability (md)	Capillary Pressure Measurement Technique
3-22	6.2	0.0120	HPPP, VD, MICP
3-40	11.2	0.0550	HPPP, VD
5-16	2.4	0.0015	VD, MICP
6-21	6.7	0.0007	HPPP, VD
8-21	10.6	0.0140	HPPP, VD, MICP

HPPP: high-pressure porous plate
 HSC: high-speed centrifuge
 MICP: high-pressure mercury injection
 VD: vapor desorption

The core samples for our study were selected using a hydraulic rock typing technique. A hydraulic rock type classification provides a physical measure of a rock's flow and storage properties at current geologic conditions. Figure 2 is an example of an incremental mercury intrusion plot used to identify the range of pore throat radii observed in this tight gas sand.²¹⁻²⁴ When described on the basis of the dominant pore throat radius, we observe distinct groupings of rocks having similar flow and storage properties, *i.e.*, hydraulic rock types. These hydraulic rock type groups, as shown in Fig. 3, are linked to Figure 2 using the Pittman²⁵ method where the lines

of constant pore throat radius in Fig. 3 define the hydraulic rock type boundaries shown in Fig. 2.

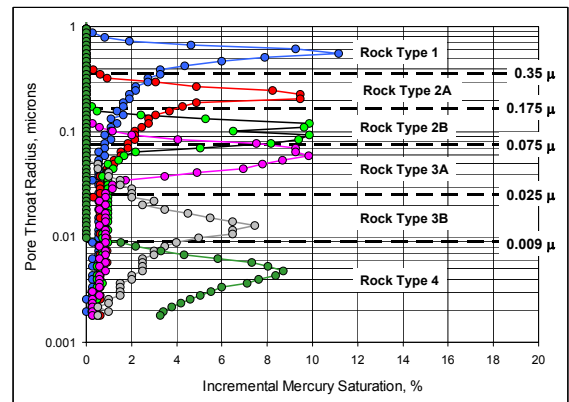


Fig. 2—Incremental mercury intrusion plot used to identify hydraulic rock types for core samples used in study.

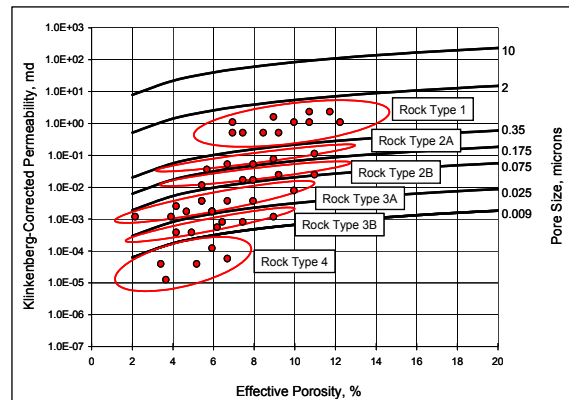


Fig. 3—Pittman plot showing range of porosity and permeability for hydraulic rock types used in study.

We sampled a range of porosities and permeabilities that we feel correspond to the most productive intervals, but we have also included some samples from less productive zones for comparison. Hydraulic rock types 1, 2A, 2B, and 3A are generally considered to be reservoir rock. Because of their low permeability, high initial water saturation and significant degree of vertical heterogeneity, rock types 3B and 4 are non-reservoir rocks and probably act as flow baffles, barriers, and seals.

Although not shown in the tables, water saturations in these rocks range from as low as 5% in hydraulic rock type 1 to about 50% in hydraulic rock type 3A. Note that both porosity and Klinkenberg-corrected permeability were obtained at a net overburden pressure of 800 psig.

General Procedures. All capillary pressures were measured using a drainage process (*i.e.*, water saturations decreasing) using an air-brine fluid system at laboratory conditions. Prior to making any measurements, the cores were cleaned and dried. We used a low-temperature azeotropic (chloroform-methanol) solution with a Dean Stark extraction process to clean the cores. The samples were then dried in a humidity-controlled environment. The purpose of these cleaning and drying protocols was to reduce or eliminate any damage or alteration of rock materials, especially the clays.

Before measuring any capillary pressure, we first saturated the cores fully with synthetic brine having a NaCl concentration of 5,000 ppm. The test sequence began by desaturating the cores and measuring capillary pressures using either the high-pressure porous plate or the high-speed centrifuge method. Although capillary pressures were usually measured at four pressure steps (i.e., 100, 200, 400 and 1000 psig), we sometimes added pressure steps to better define the curve shape.

When the pressure limits of either the high-speed centrifuge or high-pressure porous plate were reached, we then changed to the vapor desorption method to continue the desaturation process. Unlike previous measurements using the vapor desorption technique^{5,8,18-20} that used various types and concentrations of salt solutions to control vapor pressure, we used a humidity chamber to control the relative humidity, thus controlling the vapor pressure lowering process. Temperature was maintained at 30°C for all measurements. We began at the highest relative humidity and reduced the value in step-wise fashion at all subsequent measurements. This particular test sequence also represents a drainage type test where the wetting phase saturation is reduced as the humidity of the chamber is reduced, resulting in an increase in the computed capillary pressure. Core samples were weighed periodically to determine when equilibrium water saturation was achieved at each relative humidity step. Water saturation was determined by gravimetric techniques, and capillary pressure was computed using the classic form of the Kelvin equation.⁵

High-pressure, mercury injection capillary pressure (MICP) testing was the last set to be completed due to the destructive nature of this test. Drainage capillary pressure measurements were completed using a 117-pressure-step protocol—25 pressure steps in the low-pressure chamber (below atmospheric) and 92 pressure steps in the high-pressure chamber—corresponding to a measured capillary pressure range of 0 psig to 60000 psig. All mercury data were conformance corrected for surface sample roughness. Moreover, we also employed two different commercial laboratories who conducted the MICP tests using either the no-blank or blank correction options. Our goal was to assess the influence of total system compressibility on the capillary pressure and wetting phase saturation distribution. Finally, the MICP were converted to an air-brine system at laboratory conditions for comparison to data from the other techniques.

Continuity Between Vapor Desorption and High-Speed Centrifuge/High-Pressure Porous Plate Data

Because of their upper pressure limitations (approximately 1000 psia), neither the high-speed centrifuge nor high-pressure porous plate techniques are always applicable in the high capillary pressure range, especially for tight gas sands. Likewise, the vapor desorption technique may have limited applications in the higher water saturation range for low-permeability rocks. Therefore, we have combined several techniques in an attempt to cover the entire range of water saturation space.

Figures 4 and 5 are Cartesian and semilog plots, respectively, showing comparisons of capillary pressure measurements from the vapor desorption and high-speed centrifuge methods for samples from Well No. 1, North

Louisiana Field. Several previous studies^{5,8,18} comparing capillary pressures obtained from different methods show some overlap between capillary pressures obtained with different methods. Although we do not see any such overlap in our data, we do observe a very clear and obvious continuity trend between the centrifuge measurements at 1,000 psig and vapor desorption data at 2,000 psig. This data continuity trend is much more apparent in the semilog (Fig. 5) than the Cartesian plot.

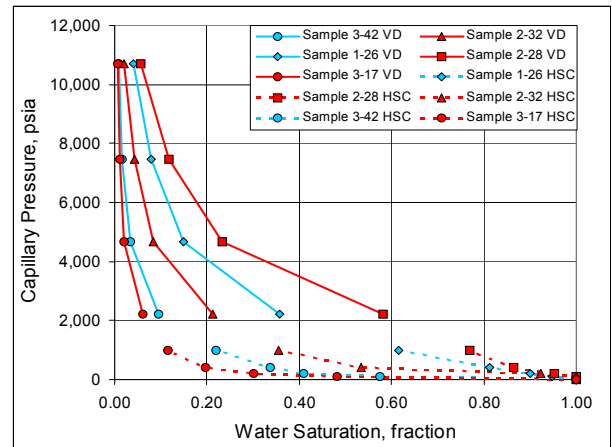


Fig. 4—Cartesian plot comparing capillary pressures from vapor desorption (VD) and high speed centrifuge (HSC) techniques, North Louisiana Field Well No. 1.

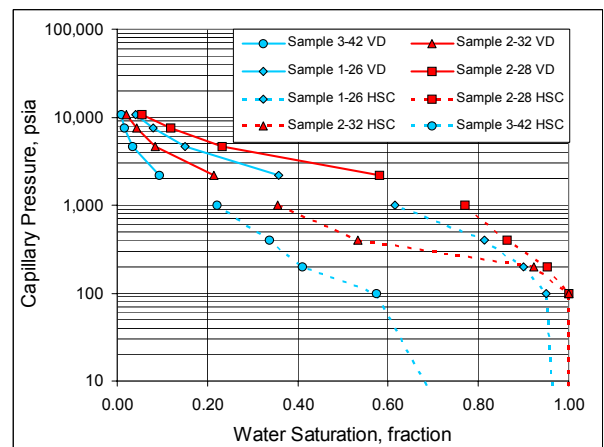


Fig. 5—Semilog plot comparing capillary pressures from vapor desorption (VD) and high speed centrifuge (HSC) techniques, North Louisiana Field Well No. 1.

Similarly, Figures 6 and 7 are Cartesian and semilog plots, respectively showing comparisons of capillary pressure measurements from the vapor desorption and high-pressure porous plate methods for many of the same core samples tested in Figs. 4 and 5. We observe the same continuity trend between the porous plate upper pressure and the vapor desorption lower pressure end points.

Figures 8 and 9 are additional Cartesian and semilog plots, respectively, of capillary pressure measurements from the vapor desorption and high-speed centrifuge methods for core samples from Well No. 1, East Texas Field 1. Like the data shown in Figs. 4-7 for the core samples from the North Louisiana Field, continuity between data from the two

methods is clearly evident. We also note the differences between the capillary pressure curve shapes and characteristics for the three wells shown in Figs. 4-9. Most of the differences probably reflect variations in the hydraulic rock types shown in Figs. 2 and 3.

Although not shown, we observed similar results with the data from other wells. Moreover, the capillary pressures from all wells appear to follow a consistent trend, thus providing excellent drainage curves spanning the complete saturation and capillary pressure range. Note also that we were able to achieve air-brine capillary pressures in excess of 10,000 psi and water saturations below 10% with the vapor desorption method. This achievement is quite important in tight gas sands similar to the Lower Cotton Valley/Bossier sands which are characterized by ultra-low connate water saturations associated with high capillary pressures.¹

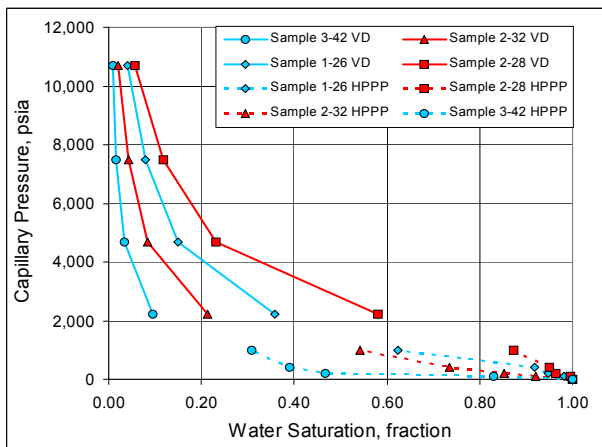


Fig. 6—Cartesian plot comparing capillary pressures from vapor desorption (VD) and high-pressure porous plate (HPPP) techniques, North Louisiana Field Well No. 1.

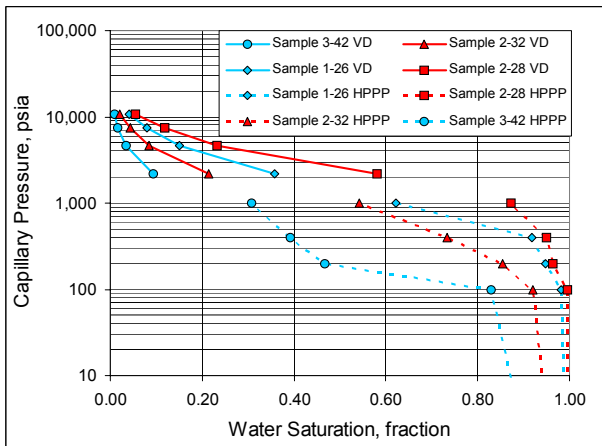


Fig. 7—Semilog plot comparing capillary pressures from vapor desorption (VD) and high-pressure porous plate (HPPP) techniques, North Louisiana Field Well No. 1.

Comparison of High-Pressure Mercury Injection to Composite Capillary Pressure Data

In this section, we compare high-pressure, mercury injection capillary pressures (MICP) to composite curves constructed from combinations of vapor desorption/high-speed centrifuge and vapor desorption/high-pressure porous plate data. Use of

composite curves allows us to compare the MICP data over the entire water saturation range. An additional objective of these comparisons was to assess the accuracy of the MICP data. Since the MICP method uses two non-wetting fluids to generate capillary pressures, the accuracy of mercury injection is often questioned. Conversely, we would anticipate that the composite capillary pressure data, which are generated using reservoir-like fluids, would more accurately describe the capillary pressure characteristics.

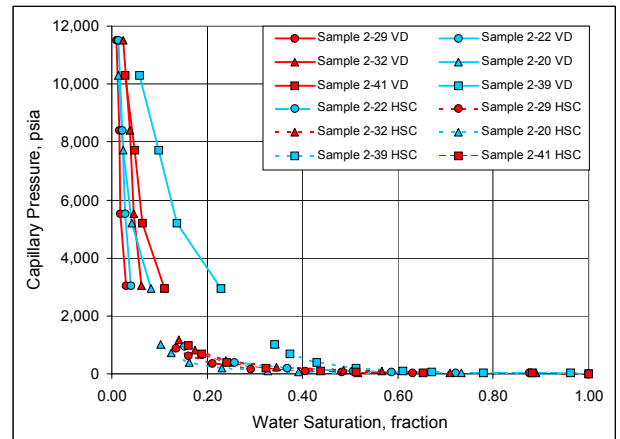


Fig. 8—Cartesian plot comparing capillary pressures from vapor desorption (VD) and high speed centrifuge (HSC) techniques, East Texas Field 1 Well No. 1.

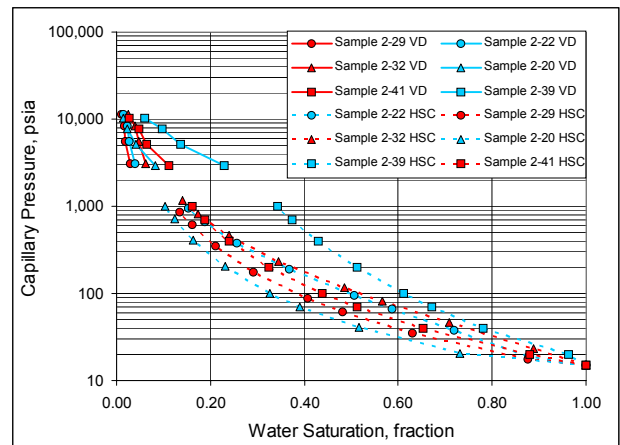


Fig. 9—Semilog plot comparing capillary pressures from vapor desorption (VD) and high speed centrifuge (HSC) techniques, East Texas Field 1 Well No. 1.

Figures 10 and 11 are Cartesian and semilog plots, respectively, illustrating the comparison between MICP and the composite vapor desorption/high-speed centrifuge data for the North Louisiana Field, Well No. 1. The mercury data were conformance corrected (low-pressure end point), but were not blank corrected (high-pressure end point). All capillary curves are also converted to an air-brine system at laboratory conditions for direct comparison to the vapor desorption, high-speed centrifuge, and high-pressure porous plate data.

Inspection of the Cartesian plot in Fig. 10 shows that both MICP and the composite capillary pressure data have the same general curve shape, particularly in the lower wetting phase

region. Except for sample 3-42, the MICP data tend to indicate lower irreducible water saturations. Similarly, in the higher water saturation range shown in Fig. 11, both the MICP and composite curve data also have the same general shape. However, the MICP not only exhibit a definitively higher displacement pressure, but also predict higher water saturations than the composite curve for a given capillary pressure.

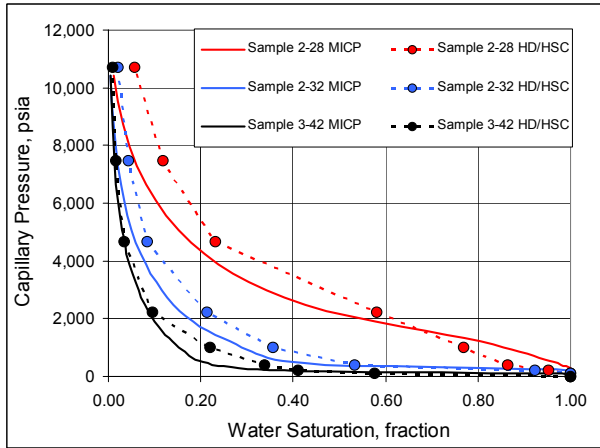


Fig. 10—Cartesian plot comparing high-pressure mercury injection capillary pressures (MICP) to composite vapor desorption/high speed centrifuge data (HD/HSC), North Louisiana Field Well No. 1.

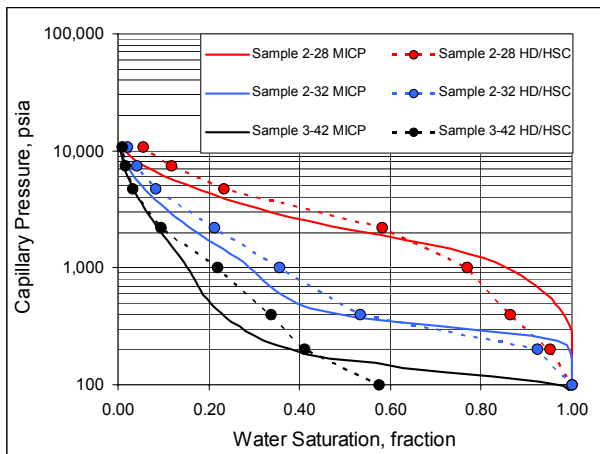


Fig. 11—Semilog plot comparing high-pressure mercury injection capillary pressures (MICP) to composite vapor desorption/high speed centrifuge data (HD/HSC), North Louisiana Field Well No. 1.

We also evaluated composite capillary pressure curves constructed with data from the high-pressure porous plate method. Figures 12 and 13 are additional Cartesian and semilog plots, respectively, illustrating the comparison between MICP and the composite vapor desorption/high-pressure porous plate data for Well No. 1, East Texas Field No. 2. As discussed previously, the mercury data were conformance corrected, but were not blank corrected for this comparison.

We observe similar differences between the MICP and composite capillary pressure using the high-pressure porous plate. Both samples shown in the Cartesian plot in Fig. 12 indicate a lower irreducible water saturation. Unlike the

capillary pressure data shown in Fig. 11 in the high water saturation range, the MICP and composite data show good agreement. Although not shown, we observed a similar range of differences for the other core samples evaluated in our study.

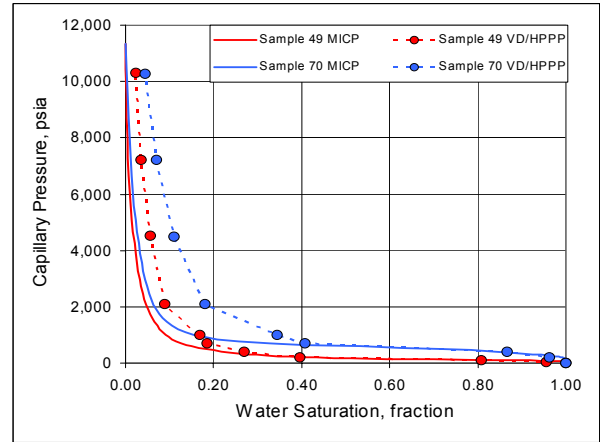


Fig. 12—Cartesian plot comparing high-pressure mercury injection capillary pressures (MICP) to composite vapor desorption/high-pressure porous plate data (HD/HPPP), East Texas Field 2 Well No. 1.

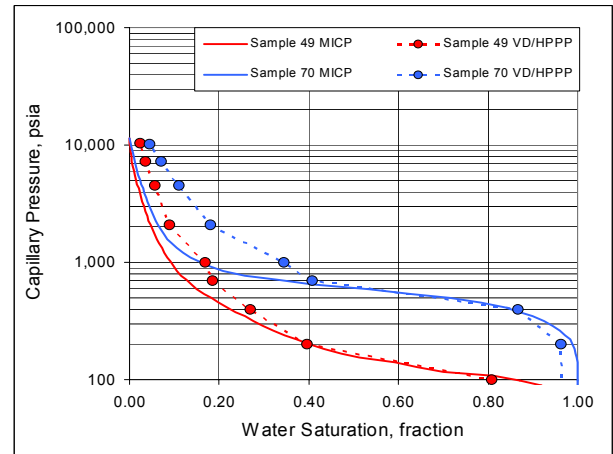


Fig. 13—Semilog plot comparing high-pressure mercury injection capillary pressures (MICP) to composite vapor desorption/high-pressure porous plate data (HD/HPPP), East Texas Field 2 Well No. 1.

As we noted previously, a significant advantage of the vapor desorption, centrifuge, and porous plate methods is the ability to use reservoir fluids. In fact, these methods can also be used to evaluate core samples under native-state conditions. In contrast, the MICP method uses two non-wetting fluids—air and mercury—to measure capillary pressures.

Furthermore, air is implicitly assumed to be the wetting phase when the laboratory data are converted to reservoir conditions. Consequently, one source of the MICP inaccuracies may be related to an incorrect laboratory model of the reservoir rock wetting conditions. Another source may be attributed to the blank correction which affects the test results at high pressures. We will evaluate the effects of the blank correction in the next section.

Influence of Conformance and Blank Corrections on MICP Data

The two most likely sources of error in MICP measurements are caused by mercury conformance at low pressures and system compressibility at high pressures.²⁶ Unfortunately, there are no published industry standards for correcting either of these errors. The conformance correction, which is also frequently called closure, is a function of the mercury volume required to fill the external voids and surface irregularities on a core sample. The high contact angle and non-wetting characteristics of mercury require an applied pressure to initiate the injection process. External vugs or irregularities that fill initially at very low pressures are not necessarily indicative of the sample entry or displacement pressure and should be removed from the injection volume. Consequently, the conformance correction focuses on the data in the low-pressure region.

The second source of error is from compressibility of the equipment elements, including the mercury, the glass penetrometer (sample holder), the oil bath used for creating the pressure, and the system frame. Of these, it is thought²⁶ that the mercury compressibility contributes the greatest amount of error and that the greatest amount of compression will occur at high pressure. The correction associated with this error is called the blank correction. There are numerous methods being practiced by commercial laboratories. These range from performing mercury injection with an empty penetrometer to performing an injection run on a synthetic cylinder of quartz (*i.e.*, a 'blank') within the penetrometer. Note that this 'blank' cylinder has no pores, so any measured mercury 'displacement' is thought to be related to only the total system expansion and compression.

To evaluate the effects of the conformance and blank corrections, we compare MICP data computed in two different ways: uncorrected and both blank and conformance corrected. Two different cumulative mercury injection curves are shown in Figure 14. Note that the conformance correction affects the low-pressure region by shifting the capillary pressure curve towards the higher wetting phase saturations. Conversely, the blank correction affects the high-pressure region by shifting the curves towards lower wetting phase saturations. Both corrections affect all of the study samples in the same way but with varying magnitudes of wetting phase saturation offset.

To illustrate the effect of the blank correction, we compare three pairs of mercury injection curves representing three different hydraulic rock types (Fig. 15). Each of the curves has the low-pressure conformance correction. However, one curve in each pair has no high-pressure blank correction, while the other curve in each pair includes the blank correction. Inspection of Fig. 15 shows that the blank correction shifts the capillary pressure data to a lower water saturation than without the correction.

We also observe that the best hydraulic rock type (black data points) is affected more by the blank correction than is the worst hydraulic rock type (red data points). The best hydraulic rock type has a larger pore volume (and greater permeability) requiring more mercury injection volume to completely flood all the pores. Since mercury compressibility causes the largest error in the overall system, then we would

expect a larger volume of mercury to require a larger blank correction.

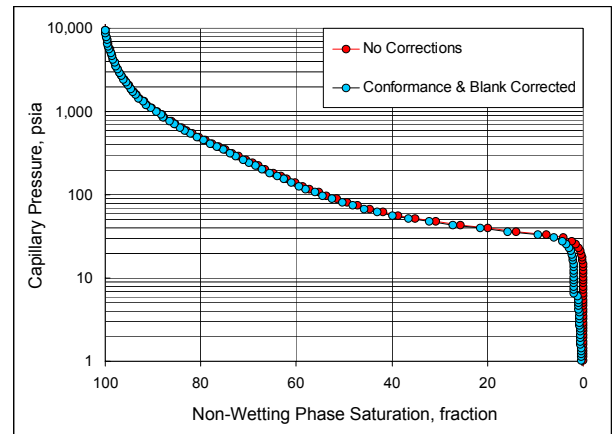


Fig. 14—Semilog plot of MICP data comparing effects of both blank and conformance corrections on the capillary pressures.

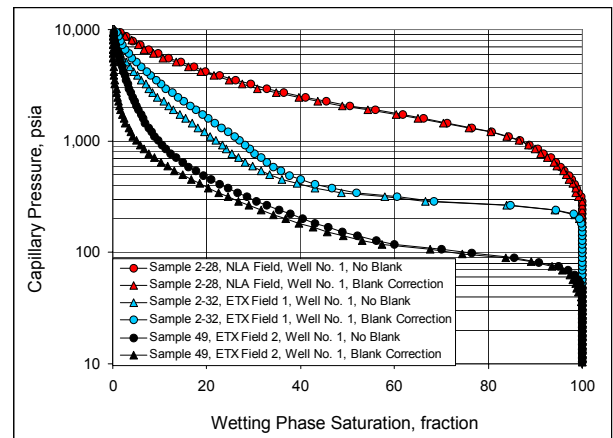


Fig. 15—Semilog plot of three pairs of MICP data comparing effects of no blank vs. blank corrections on the curve shape and characteristics.

Recall that the MICP curves shown in Figures 10-13 had no high-pressure blank corrections. If, however, the blank corrections had been applied, then we would have observed even larger differences when compared to the composite capillary pressures data. For this reason, we chose not to include the blank corrections. The next section will document a method for normalizing or calibrating the MICP data to a reference set of vapor desorption curves. This calibration process will correct the MICP data, thus generating more accurate mercury data.

Calibrating MICP Data Using Vapor Desorption Data in the Low Water Saturation Region

This study has documented significant differences between the MICP data and the composite capillary pressure curves constructed from a combination of vapor desorption, centrifuge, and porous plate methods. Because the tests use true wetting and non-wetting fluids (*i.e.*, brine and air), we consider the composite capillary pressure data to be more representative of the reservoir, and therefore more accurate. Further, we believe the differences between the MICP data

and the composite curves may be caused by the fluids used to generate the data and their wetting characteristics.

Recall that the mercury injection method uses an air-mercury system in which mercury displaces air during the injection process. Since this test is considered to be a drainage process (*i.e.*, the wetting phase saturation is decreasing), then air must be regarded as the wetting phase. In fact, neither air nor mercury is a true rock wetting fluid under any condition. Unfortunately, mercury injection is frequently used, especially in tight gas sands. Therefore, we propose a method to calibrate or match the MICP curves using the vapor desorption data. This calibration process will not only allow us to salvage existing or legacy MICP data, but will also provide more accurate MICP data to define the reservoir fluid saturation distribution. The basis of the calibration is a simple conversion of the air-mercury data to air-brine using the following equation

$$P_{cAW} = P_{cAM} \left(\frac{2\sigma_{AW} \cos \theta_{AW}}{2\sigma_{AM} \cos \theta_{AM}} \right) \dots\dots\dots (4)$$

where

- P_{cAW} = pseudo air-water capillary pressure
- P_{cAM} = air-mercury capillary pressure
- σ_{AW} = air-water surface tension
- σ_{AM} = air-mercury surface tension
- θ_{AW} = air-water contact angle
- θ_{AM} = air-mercury contact angle

To illustrate the process, we calibrated the MICP curves for several data sets from the North Louisiana Field, Well Nos. 1 and 2 (Figs. 16 and 17, respectively). We adjusted the MICP data by decreasing the $\sigma\cos\theta$ term of the air-mercury system until the mercury curves matched the vapor desorption curves. To get the best match between the MICP and the vapor desorption data required that we use different adjustment factors for each data set. Note that, although each data set represents a range of hydraulic rock types, we used constant adjustment factors for each core sample.

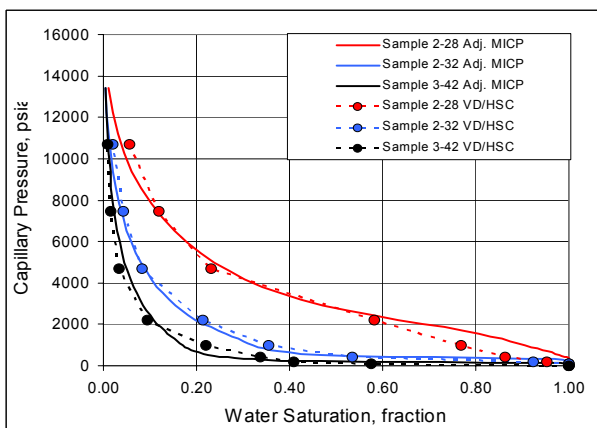


Fig. 16—Cartesian plot comparing best match between composite vapor desorption/high-speed centrifuge (VD/HSC) and calibrated mercury injection (MICP) data, North Louisiana Field, Well No. 1.

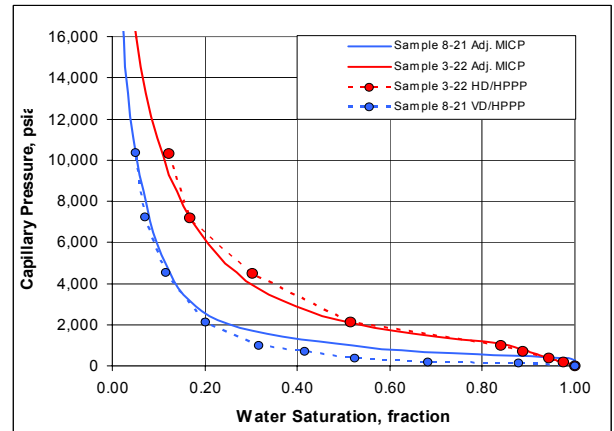


Fig. 17—Cartesian plot comparing best match between composite vapor desorption/high-pressure porous plate (VD/HPPP) and calibrated mercury injection (MICP) data, North Louisiana Field, Well No. 2.

The basis of the MICP normalization or calibration is the belief that the differences between the MICP data and the composite curves may be caused by the fluids used to generate the MICP data and their wetting characteristics. Figure 18 illustrates the conceptual model used to explain the calibration process. The two circles on the left side of the diagram symbolize sand grains from a MICP test. Note that there is no fluid wetting the surfaces since neither air nor mercury is a true wetting fluid.

To match the vapor desorption data, we adjust the air-mercury $\sigma\cos\theta$ term, thus shifting the MICP data to the higher wetting phase saturations. Essentially, we are converting the air-mercury data with no true wetting fluids to an equivalent air-brine system with a wetting phase (*i.e.*, water) by “numerically wetting” the data. As illustrated by the two circles on the right side of the plot that now have a continuous wetting phase coating the sand grains, we compute a “pseudo” capillary pressure corresponding to the higher wetting phase region.

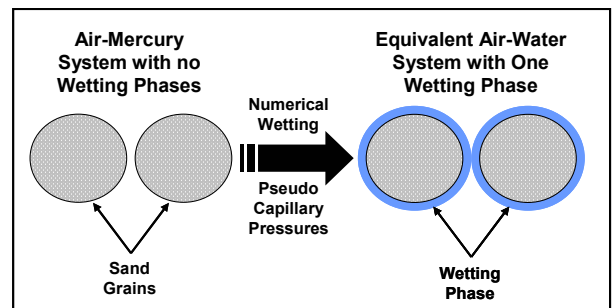


Fig. 18—Conceptual physical model illustrating conversion of MICP data with no true wetting phases to pseudo-capillary pressure data with a wetting phase.

Summary and Conclusions

We have conducted a laboratory study comparing capillary measurement techniques for tight gas sands. We evaluated the more traditional high-speed centrifuge and high-pressure mercury injection methods as well as the less conventional high-pressure porous plate and vapor desorption techniques. On the basis of our study, we offer the following conclusions:

1. For the range of hydraulic rock types tested in our study, we observed a very clear and obvious continuity trend between the porous plate and centrifuge upper pressure end points (about 1,000 psig) and the vapor desorption lower pressure end point (about 2,000 psig). Although we did not observe any overlap between the data, the excellent continuity gives us confidence in the vapor desorption measurement technique.
2. The results of our study show significant differences between the mercury injection data and the composite capillary pressure curves constructed with data from the other vapor desorption, high-speed centrifuge and high-pressure porous plate methods. The most likely source of these errors may be the fluids used to generate the MICP data and their non-wetting characteristics.
3. In general, the MICP capillary pressure tests generate saturation distributions that are consistently lower than that computed by the composite curves. This difference is especially apparent in the low saturation range where the MICP data may significantly underestimate the irreducible water saturation. We did not observe any consistent trend in the high water saturation range.
4. Because of the differences between the MICP and composite curve data, we have concluded that high-pressure mercury injection can be used to quantify pore size distribution, but often inaccurately characterizes capillary pressures, particularly the irreducible water saturation.
5. Inclusion of a high-pressure blank correction for the MICP data tends to exacerbate the differences between the mercury injection capillary pressures and the composite curves. The differences appear to be larger for the better reservoir quality hydraulic rock types, *i.e.*, samples with larger porosity and permeability.
6. Because the tests use true wetting and non-wetting fluids (*i.e.*, brine and air), we believe the composite capillary pressure data, constructed from a combination of the vapor desorption data for the low water saturation range and high-speed centrifuge or high-pressure porous plate data for the high water saturation range, to be more representative of the reservoir, and therefore more accurate.
7. We propose a method to calibrate or match the MICP curves using the vapor desorption data. This calibration process will not only help salvage legacy MICP data, but will also provide more accurate MICP data to define the reservoir fluid saturation distribution.

r	=	capillary radius
RH	=	relative humidity
R	=	universal gas constant
T	=	absolute temperature
V_m	=	molar volume of water
σ	=	interfacial tension
σ_{AW}	=	air-water surface tension
σ_{AM}	=	air-mercury surface tension
θ	=	contact angle
θ_{AW}	=	air-water contact angle
θ_{AM}	=	air-mercury contact angle

Acknowledgments

We would like to express our thanks to the management of Anadarko Petroleum Corporation for their support and for permission to publish the results of our study. We would also like to acknowledge OMNI Laboratories, Inc. for their excellent work and collaborative efforts.

References

1. Newsham, K.E. and Rushing, J.A.: "Laboratory and Field Observations of an Apparent Sub Capillary-Equilibrium Water Saturation Distribution in a Tight Gas Sand Reservoir," paper SPE 75710 presented at the 2002 SPE Gas Technology Symposium, Calgary, Alberta, Canada, April 5-8.
2. Newsham, K.E., Rushing, J.A., and Lasswell, P.M.: "Use of Vapor Desorption Data to Characterize High Capillary Pressures in a Basin-Centered Gas Accumulation with Ultra-Low Connate Water Saturations," paper SPE 84596 presented at the 2003 SPE Annual Technical Conference and Exhibition, Denver CO, Oct. 5-8.
3. Collins, R.E.: *Flow of Fluids Through Porous Materials*, The Petroleum Publishing Co., Tulsa, OK (1976), pp 33-36.
4. Amyx, J.W., Bass, D.M., Jr., and Whiting, R.L.: *Petroleum Reservoir Engineering: Physical Properties*, McGraw-Hill Book Co., New York, NY (1960).
5. Melrose, J.C.: "Use of Water Vapor Desorption Data in the Determination of Capillary Pressure," paper SPE 16286 presented at the 1987 SPE International Symposium on Oilfield Chemistry, San Antonio, TX, Feb. 4-6.
6. Calhoun, J.C., Jr., *et al.* "Experiments on the Capillary Properties of Porous Solids," *Trans. AIME*, vol. 186 (1949), pp 189-196.
7. Thomson, W. (Lord Kelvin), "On the Equilibrium of Vapour at a Curved Surface of Liquid," *Proc., Roy. Soc. Edinburgh*, 1870, 7, 63-67; *Phil. Mag.* (1871), Ser. 4, 42, 448-452.
8. Melrose, J.C.: "Valid Capillary Pressure Data at Low Wetting-Phase Saturation," *SPE Reservoir Engineering* (Feb. 1990), pp 95-100.
9. McCullough, F.W., *et al.*: "Determination of the Interstitial-Water Content of Oil and Gas Sand by Laboratory Tests of Core Samples," *Drill. & Prod. Prac. API* (1944), pp 180-188.
10. Thornton, O.F. and Marshall, D.L.: "Estimating Interstitial Water by the Capillary Pressure Method," *Trans. AIME*, vol. 170 (1947), pp 69-80.
11. Bruce, W.A. and Welge, H.J.: "Restored-State Method for Determination of Oil-in-Place and Connate Water," *Oil & Gas J.*, vol. 46 (1947), pp 22-23.
12. Rose, W. and Bruce, W.A.: "Evaluation of Capillary Character in Petroleum Reservoir Rock," *Trans. AIME*, vol. 186 (1949), pp 127-142.
13. Hassler, G.L. and Brunner, E.: "Measurement of Capillary Pressures in Small Core Samples," *Trans. AIME*, vol. 160 (1945), pp 113-144.

Nomenclature

P_c	=	capillary pressure
P_{nw}	=	pressure of the non-wetting phase
P_w	=	pressure of the wetting phase
p_2	=	partial vapor pressure for brine within the sample
p_4	=	partial vapor pressure for salt solution
P_{cAW}	=	pseudo air-water capillary pressure
P_{cAM}	=	air-mercury capillary pressure

14. Slobod, R.L., *et al.*: "Use of Centrifuge for Determining Connate Water, Residual Oil, and Capillary Pressure Curves of Small Core Samples," *Trans. AIME*, vol. 192 (1951), pp 127-134.
15. O'Meara, D.J., Jr., *et al.*: "Centrifuge Measurements of Capillary Pressure: Part 1-Outflow Boundary Condition," paper SPE 18296 presented at the 1988 SPE Annual Technical Conference and Exhibition, Houston, TX, October 2-5.
16. Hirasaki, G.J., *et al.*: "Centrifuge Measurements of Capillary Pressure: Part 1-Cavitation," paper SPE 18592 presented at the 1988 SPE Annual Technical Conference and Exhibition, Houston, TX, October 2-5.
17. Purcell, W.R.: "Capillary Pressures-Their Measurement Using Mercury and the Calculation of Permeability Therefrom," *Trans. AIME*, vol. 186 (1949), pp 39-48.
18. Melrose, J.C., Dixon, J.R., and Malison, J.E.: "Comparison of Different Techniques For Obtaining Capillary Pressure Data In the Low Saturation Range," paper SPE 22690 presented at the 1991 SPE Annual Technical Conference and Exhibition, Dallas, TX, Oct. 6-9.
19. Morrow, N.R., Brower, K.R., and Kilmer, N.H.: "Relationships of Pore Structure to Fluid Behavior in Low Permeability Gas Sands", Final Report, DOE/BC/10216-13 (DE84012721), U.S. Dept. of Energy, Bartlesville (Sept., 1984), 60-71.
20. Ward, J.S., and Morrow, N.R.: "Capillary Pressure and Gas Relative Permeabilities of Low Permeable Sandstone", paper SPE/DOE 13882 presented at the 1985 SPE/DOE Symposium on Low Permeability Reservoirs, Denver, CO, May, 1985.
21. Washburn, E. W.: "Note On A Method of Determining the Distribution of Pore Sizes In A Porous Material", *Proc.*, The National Academy of Science (1921), v. 7, p.115-116.
22. Gunter, G.W., *et al.*: "Early Determination of Reservoir Flow Units Using an Integrated Petrophysical Model", Paper SPE 38679 presented at the 1997 SPE Annual Technical Conference and Exhibition, San Antonio, TX, October 5-8.
23. Newsham, K.E. and Rushing, J.A.: "An Integrated Work-Flow Model to Characterize Unconventional Gas Resources: Part I-Geological Assessment and Petrophysical Evaluation," paper SPE 71351 presented at the 2001 SPE Annual Technical Conference and Exhibition, New Orleans, LA, September 30-October 3.
24. Rushing, J.A. and Newsham, K.E.: "An Integrated Work-Flow Model to Characterize Unconventional Gas Resources: Part II-Formation Evaluation and Reservoir Modeling," paper SPE 71352 presented at the 2001 SPE Annual Technical Conference and Exhibition, New Orleans, LA, September 30-October 3.
25. Pittman, E. D.: "Relationship of Porosity and Permeability to Various Parameters Derived From Mercury Injection-Capillary Pressure Curves for Sandstone", *AAPG Bull.*, (Feb. 1992), v. 76, No. 2, p. 191-198.
26. Webb, P.A.: "An Introduction To The Physical Characterization of Materials by Mercury Intrusion Porosimetry With Emphasis On Reduction and Presentation of Experimental Data", Micromeritics Corp Internal Publication, Norcross, GA, 2001.